TECHNICAL RESEARCH REPORT

Sampled-Data Modeling and Analysis of the Power Stage of PWM DC-DC Converters

by Chung-Chieh Fang, Eyad H. Abed

T.R. 99-25

ISR
INSTITUTE FOR SYSTEMS RESEARCH

Sampled-Data Modeling and Analysis of the Power Stage of PWM DC-DC Converters

Chung-Chieh Fang and Eyad H. Abed
Department of Electrical and Computer Engineering
and the Institute for Systems Research
University of Maryland
College Park, MD 20742 USA

Abstract

The power stage of the PWM DC-DC converter is modeled and analyzed using the sampled-data approach. The work addresses continuous and discontinuous conduction mode under voltage mode control, and continuous conduction mode under current mode control. For each configuration, nonlinear and linearized sampled-data models, and control-to-output transfer function are derived. Using this approach, both current mode control and discontinuous conduction mode can be handled systematically in a unified framework, making the modeling for these cases simpler than with the use of averaging. The results of this paper are similar to results of Tymerski, but they are presented in a simpler manner tailored to facilitate immediate application to specific circuits. It is shown how sampling the output at certain instants improves the obtained phase response. Frequency responses obtained from the sampled-data model are more accurate than those obtained from various averaged models. In addition, a new ("lifted") continuous-time switching frequency-dependent model of the power stage is derived from the sampled-data model. Detailed examples illustrate the modeling tools presented here, and also provide a means of comparing results obtained from the sampled-data approach with those obtained from averaging.

1 Introduction

Recently there has been intensive research on modeling and analysis of the *power stages* of the PWM DC-DC converter [1, 2, 3, 4, 5, 6, 7, 8, 9, 10, 11, 12], especially in special configurations such as under current mode control [13, 14, 15, 16, 17, 18, 11] and in discontinuous conduction mode [19, 20, 21, 22]. The better the power stage is modeled, the better closed-loop performance can be achieved as expected. Among different modeling approach, averaging method is the most popular one. However, the important work by Tymerski in [7, 8], which uses time-varying system theory to derive power stage dynamics, did not get much attention.

1

In this paper, the power stage is modeled and analyzed using the sampled-data approach [23, 24, 25, 26, 27, 28]. This work complements the authors' work [27, 29] which develops sampled-data models and analysis for the *closed-loop* PWM DC-DC converter. The work addresses continuous and discontinuous conduction mode under voltage mode control, and continuous conduction mode under current mode control. For each configuration, *analytical* nonlinear and linearized sampled-data models, and the control-to-output transfer function are derived. Using this approach, both current mode control and discontinuous conduction mode can be handled systematically in a unified framework, making the modeling for these cases simpler than with the use of averaging. The results of this paper are similar to the work by Tymerski [7, 8], but they are presented in a simpler manner tailored to facilitate immediate application to specific circuits. It is shown how sampling the output at certain instants improves the obtained phase response. Frequency responses obtained from the sampled-data model are more accurate than those obtained from various averaged models. In addition, a new ("lifted") continuous-time switching frequency-dependent model of the power stage is derived from the sampled-data model. Examples illustrate the increased accuracy of controls designed using the new power stage models.

In this work, the *orbital* nature of operating condition is emphasized. This differs from the averaging method, which averages the periodic steady state of a PWM converter to an equilibrium. The periodic steady state in high switching operation has small amplitude (ripple), and averaging is therefore a reasonable approach. However, close to the onset of instability, the *periodic* nature of the steady state operating condition needs to be considered in order to obtain accurate results. The inherent dynamics for a periodic solution and an equilibrium are different. This issue is generally neglected in most power electronics literature. It has been reported that the averaged models do not accurately predict subharmonic instability [2], chaotic phenomena [30, 31, 32, 33], and steady-state DC offset [10]. Moreover, it has been found that the directly obtained averaged models are inaccurate for converters operated under current mode control or in discontinuous-conduction mode. This has necessitated efforts to obtain more accurate averaged models for such cases. In contrast, sampled-data modeling can be applied systematically to converters operated both under

current mode control or in discontinuous-conduction mode and gives more accurate description about the operations of PWM DC-DC converters.

The organization of the paper is as follows. In Section 2, the power stage in continuous conduction mode (CCM) under voltage mode control is studied. The steps of sampled-data approach in [29] are followed in details. In Section 3 and 4, the power stages in discontinuous conduction mode (DCM) under voltage mode control, and CCM under current mode control, respectively, are studied. In Section 5, a new approach to derive linear continuous-time models of PWM converter power stage from sampled-data models is proposed. In Section 6, four illustrative examples are given. It is shown that the sampled-data models give a superior prediction of closed-loop performance as compared to the averaging method.

2 Continuous Conduction Mode (CCM) under Voltage Mode Control

2.1 Block Diagram Model

Consider the cycle $t \in [nT, (n+1)T]$. A block diagram model of the power stage of a PWM converter operated in CCM under voltage mode control is shown in Fig. 1, where $d_n \in \mathbf{R}$ is the switching instant within the cycle and is used as the control variable, $A_1, A_2 \in \mathbf{R}^{N \times N}$, $B_1, B_2 \in \mathbf{R}^{N \times 1}$, $E_1, E_2 \in \mathbf{R}^{1 \times N}$, are constant matrices, T is the constant switching period (inverse of switching frequency f_s), and v_s, $v_o \in \mathbf{R}$ are the source and output voltages, respectively.

2.2 Nonlinear Sampled-Data Model

Generally in the PWM converter, the switching frequency is sufficiently high that the variations in v_s in a cycle can be neglected. Take v_s to be constant within the cycle and denote it as v_{sn}. The notation v_{sn}, instead of $v_{s,n}$, is used for brevity. This notation applies to other variables. Let $x_n = x(nT)$ and $v_{on} = v_o(nT)$. The two matrices E_1 and E_2 need not be the same. For example, they can differ if the equivalent series resistance (ESR) $R_c \neq 0$. When they differ, the output
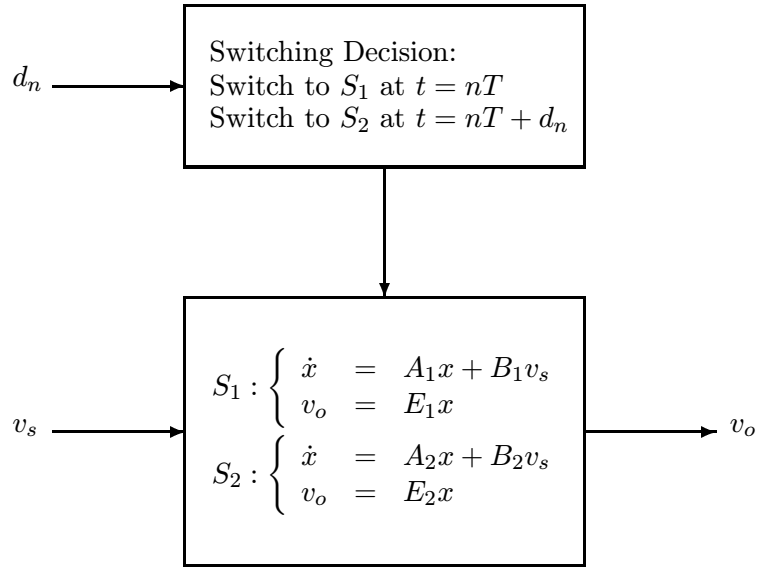
Figure 1: Power stage of PWM converter in CCM under voltage mode control

voltage is discontinuous. An example of a discontinuous output voltage waveform is shown in Fig. 2. In most applications, the output voltage of interest is the maximum, minimum, or average voltage. So in the following, E is used to denote either E_1, E_2, or $(E_1 + E_2)/2$.
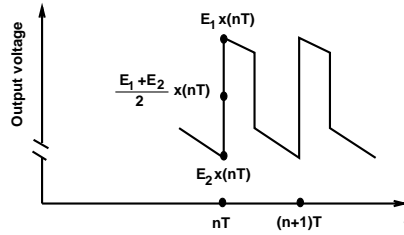

Figure 2: A discontinuous output voltage waveform

From the operation in Fig. 1, the sampled-data dynamics of the power stage is

$$
\begin{aligned}
x_{n+1} &= f(x_n, v_{sn}, d_n) \\
&= e^{A_2(T-d_n)}\left(e^{A_1 d_n} x_n + \int_0^{d_n} e^{A_1\sigma} d\sigma B_1 v_{sn}\right) + \int_0^{T-d_n} e^{A_2\sigma} d\sigma B_2 v_{sn} \quad (1) \\
v_{on} &= E x_n \quad (2)
\end{aligned}
$$

4

2.3   Steady State Analysis

A T-periodic solution $x^0(t)$ for the system in Fig. 1 corresponds to a fixed point $x^0(0)$ of the sampled-data model. The fixed point $(x_n, v_{sn}, d_n) = (x^0(0), V_s, d)$, if it exists, must satisfy

$$
\begin{aligned}
x^0(0) &= f(x^0(0), V_s, d) \\
&= e^{A_2(T-d)}\left(e^{A_1 d}x^0(0) + \int_0^d e^{A_1\sigma}d\sigma B_1 V_s\right) + \int_0^{T-d} e^{A_2\sigma}d\sigma B_2 V_s
\end{aligned}
\tag{3}
$$

Let the nominal (set-point) output voltage be V_{SET}. Assume there is little variation in $x^0(t)$ for $t \in [0, T]$. Then

$$
Ex^0(0) = V_{\text{SET}} \tag{4}
$$

The $N+1$ equations ((3) and (4)) in $N+1$ unknowns ($x^0(0)$ and d) can be solved by Newton's method [23]. Given d, the nominal duty cycle (also called duty ratio) D_c is d/T. After obtaining $x^0(0)$ and d, a periodic solution $x^0(t)$ is obtained:

$$
x^0(t) = \begin{cases}
e^{A_1 t}x^0(0) + \int_0^t e^{A_1(t-\sigma)}d\sigma B_1 u & \text{for } t \in [0, d) \\
e^{A_2(t-d)}x^0(d) + \int_d^t e^{A_2(t-\sigma)}d\sigma B_2 u & \text{for } t \in [d, T) \\
x^0(t \bmod T) & \text{for } t \geq T
\end{cases}
\tag{5}
$$

A typical periodic solution $x^0(t)$ is shown Fig. 3, where $\dot{x}^0(d^-) = A_1 x^0(d) + B_1 u$ and $\dot{x}^0(d^+) = A_2 x^0(d) + B_2 u$ denote the time derivative of $x^0(t)$ at $t = d^-$ and d^+, respectively.
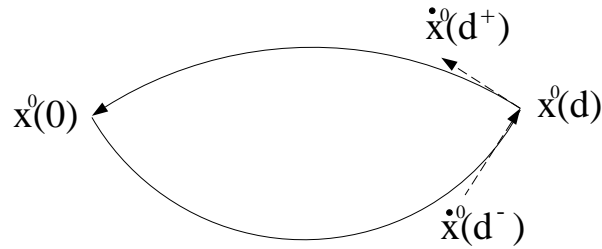

Figure 3: A typical periodic solution $x^0(t)$ of a PWM converter in state space

2.4 Existence of Periodic Solutions

In this subsection, the existence of periodic solutions in the power stage of Fig. 1 or equivalently the existence of fixed points in the sampled-data dynamics is studied. Assuming all of the eigenvalues of A_1 and A_2 are in the open left half of the complex plane, it follows that the matrices $I - e^{A_2(T-d)}e^{A_1 d}$ and $I - e^{A_1 d}e^{A_2(T-d)}$ are invertible [26]. From Eq. (3), $x^0(0)$ can be expressed as a function of d, denoted as $X(d)$:

$$X(d) := (I - e^{A_2(T-d)}e^{A_1 d})^{-1}(e^{A_2(T-d)} \int_0^d e^{A_1 \sigma} d\sigma B_1 V_s + \int_0^{T-d} e^{A_2 \sigma} d\sigma B_2 V_s) \tag{6}$$

So the $N + 1$ equations, (3) and (4), reduce to one equation in one unknown d:

$$EX(d) = V_{\text{SET}} \tag{7}$$

Next, a sufficient condition is given for the existence of a periodic solution achieving the nominal output voltage V_{SET}.

Theorem 1 *Let the nominal output voltage be V_{SET}. Assume that all of the eigenvalues of A_1 and A_2 are in the open left half of the complex plane. If*

$$(EA_2^{-1}B_2 V_s + V_{\text{SET}})(EA_1^{-1}B_1 V_s + V_{\text{SET}}) < 0 \tag{8}$$

Then there exists a periodic solution $x^0(t)$ in the power stage of Fig. 1 with $Ex^0(0) = V_{\text{SET}}$.

Proof: From Eq. (6),

$$X(0) = -A_2^{-1}B_2 V_s \tag{9}$$

$$X(T) = -A_1^{-1}B_1 V_s \tag{10}$$

From Eq. (7), if

$$(EX(0) - V_{\text{SET}})(EX(T) - V_{\text{SET}})$$
$$= (EA_2^{-1}B_2 V_s + V_{\text{SET}})(EA_1^{-1}B_1 V_s + V_{\text{SET}})$$
$$< 0$$

then by the Intermediate Value Theorem, there exists a solution d satisfying Eq. (7). Hence there exists a periodic solution $x^0(t)$. □

2.5 Linearized Sampled-Data Dynamics

When there exists a periodic solution $x^0(t)$, or equivalently a fixed point $(x^0(0), V_s, d)$, the system can be linearized at this fixed point (similar analysis has been done in [34] for the case in which A_1 and A_2 are invertible):

$$\hat{x}_{n+1} \approx \Phi_o \hat{x}_n + \Gamma_v \hat{v}_{sn} + \Gamma_d \hat{d}_n \tag{11}$$

$$\hat{v}_{on} = E\hat{x}_n \tag{12}$$

where

$$\Phi_o = \left.\frac{\partial f}{\partial x_n}\right|_\diamond = e^{A_2(T-d)} e^{A_1 d} \tag{13}$$

$$\Gamma_v = \left.\frac{\partial f}{\partial v_{sn}}\right|_\diamond = e^{A_2(T-d)} \int_0^d e^{A_1 \sigma} d\sigma B_1 + \int_0^{T-d} e^{A_2 \sigma} d\sigma B_2 \tag{14}$$

$$\Gamma_d = \left.\frac{\partial f}{\partial d_n}\right|_\diamond = e^{A_2(T-d)} ((A_1 - A_2) x^0(d) + (B_1 - B_2) V_s)$$

$$= e^{A_2(T-d)} (\dot{x}^0(d^-) - \dot{x}^0(d^+)) \tag{15}$$

(the notation $\diamond$ denotes evaluation at $(x_n, v_{sn}, d_n) = (x^0(0), V_s, d)$)

This linearized model is useful for discrete-time feedback control designs. Many different discrete-time control schemes for PWM converters have been proposed and illustrated in [26, 35].

2.6 Open-Loop Stability

The relevant stability notion is asymptotic *orbital* stability, not asymptotic stability of an equilibrium point as depicted in the averaging method. The local *open-loop* asymptotic orbital stability of the periodic solution $x^0(t)$ is determined by the eigenvalues of Φ_o. They are also open-loop poles and denoted by $\sigma[\Phi]$. The next result follows from Eq. (13).

Theorem 2 *Assume that all of the eigenvalues of at least one of A_1 and A_2 are in the open left half of the complex plane, and that neither matrix has any eigenvalue in the open right half of the complex plane. Then the periodic solution $x^0(t)$ of the power stage of Fig. 1 is asymptotically orbitally stable.*

Proof: Under the stated assumptions, the eigenvalues of Φ are inside the unit circle of the complex plane. See [26] for a detailed proof. □

2.7 A New Control-to-Output Transfer Function

Discrete-time controllers can be designed by using the linearized dynamics in (11) and (12) directly. Analog feedback control designs are generally based on the control-to-output transfer function (frequency response). From Fig. 1, control d_n is a *discrete-time* variable and output v_o is a *continuous-time* variable. One has to be careful on choosing the right time for d_n in order to correspond to the same time with v_o.

Previous works using the sampled-data modeling [36, for example] generally use the following as the control-to-output transfer function (derived from Eqs. (11) and (12))

$$\frac{\hat{v}_o(z)}{\hat{d}(z)} = E(zI - \Phi_o)^{-1}\Gamma_d \tag{16}$$

In this approach, the control (switching) exerted at $t = nT + d_n$ occurs *after* the sampling of the output at $t = nT$. This renders the model noncausal. This error in the *time* domain will cause an error in the *phase* response.

To circumvent this problem, the output $v_o(nT + d_n)$ (instead of $v_o(nT)$) is used, because the output around $t = nT + d_n$ determines the switching action. The output equation (2) now becomes

$$v_{on} = Ex(nT + d_n) = E(e^{A_1 d_n}x_n + \int_0^{d_n} e^{A_1\sigma}d\sigma B_1 v_{sn}) \tag{17}$$

with linearized dynamics

$$\hat{v}_{on} \approx E(e^{A_1 d}\hat{x}_n + \dot{x}^0(d^-)\hat{d}_n + \int_0^d e^{A_1\sigma}d\sigma B_1\hat{v}_{sn}) \tag{18}$$

8

From the linearized dynamics (11) and (18), the control-to-output transfer function is

$$T_{oc}(z) = \frac{\hat{v}_o(z)}{\hat{d}(z)} = E e^{A_1 d}(zI - \Phi_o)^{-1}\Gamma_d + E\dot{x}^0(d^-) \tag{19}$$

Given a transfer function in z domain, say $T(z)$, its effective frequency response [37, p. 93] is $T(e^{j\omega T})$, which is valid in the frequency range $|\omega| < \frac{\pi}{T}$. In the case when v_o is discontinuous because $E_1 \neq E_2$, $T_{oc}(z)$ depends on which value of E is chosen.

Compared with Eq. (16), this transfer function has an extra term $E\dot{x}^0(d^-)$. The transfer functions (16) and (19) have the same poles but different zeros. The pronounced difference between them is the phase because the output voltages are sampled at different instants. For later reference, this new approach is called the SP method and the approach which uses the sampled output at $t = nT$ is called the S method.

2.8 Open-Loop Audio-Susceptibility and Output Impedance

The effects of disturbances at the source and load on the output voltage in the *closed-loop* system are related to *open-loop* audio-susceptibility and output impedance [11]. Therefore, knowledge about the open-loop audio-susceptibility and output impedance is useful. Generally in both of them, the magnitude (but not phase) is of interest. Therefore the output equation (12) can still be used. From Eqs. (11) and (12), the open-loop audio-susceptibility is

$$T_{os}(z) = \frac{\hat{v}_o(z)}{\hat{v}_s(z)} = E(zI - \Phi_o)^{-1}\Gamma_v \tag{20}$$

To calculate the open-loop output impedance, add a fictitious current source, i_o (as perturbation), in parallel with the load. Let

$$S_1 : \dot{x} = A_1 x + B_1 v_s + B_{i1} i_o \tag{21}$$

$$S_2 : \dot{x} = A_1 x + B_2 v_s + B_{i2} i_o \tag{22}$$

where $B_{i1}, B_{i2} \in \mathbf{R}^{N \times 1}$.

9

Similar to the open-loop audio-susceptibility, the open-loop output impedance is

$$T_{oo}(z) = \frac{\hat{v}_o(z)}{\hat{i}_o(z)} = E(zI - \Phi_o)^{-1}\Gamma_i \tag{23}$$

where

$$\Gamma_i = e^{A_2(T-d)} \int_0^d e^{A_1\sigma} d\sigma B_{i1} + \int_0^{T-d} e^{A_2\sigma} d\sigma B_{i2} \tag{24}$$

3 Discontinuous Conduction Mode (DCM) under Voltage Mode Control

The modeling and analysis steps taken in Section 2 are now applied to the DCM case. For brevity, the discussion of open-loop stability and the derivation of the open-loop audio-susceptibility and output impedance are omitted.

3.1 Block Diagram Model

A general model of the power stage of a PWM converter operating in DCM under voltage mode control is shown in Fig. 4. Similar to CCM, the switching instant from S_1 to S_2 within the cycle is used as the control variable and denoted as d_{1n}. The notation d_{1n}, instead of $d_{1,n}$, is used for brevity. The matrix $F \in \mathbf{R}^{1 \times N}$ is chosen such that $Fx = i_L$. The remaining notation is as in Fig. 1.

Consider the cycle $t \in [nT, (n+1)T)$. In DCM, there are three stages in the cycle:

$$S_1 : \dot{x} = A_1 x + B_1 v_s \quad \text{for } t \in [nT, nT + d_{1n}) \tag{25}$$

$$S_2 : \dot{x} = A_2 x + B_2 v_s \quad \text{for } t \in [nT + d_{1n}, nT + d_{2n}) \tag{26}$$

$$S_3 : \dot{x} = A_3 x + B_3 v_s \quad \text{for } t \in [nT + d_{2n}, (n+1)T) \tag{27}$$

Switching from S_1 to S_2 occurs at $nT + d_{1n}$, where d_{1n} is a control variable. Switching from S_2 to S_3 occurs at $nT + d_{2n}$, where d_{2n} is determined by the inductor current when its value reaches zero, i.e., $i_L(nT + d_{2n}) = Fx(nT + d_{2n}) = 0$.
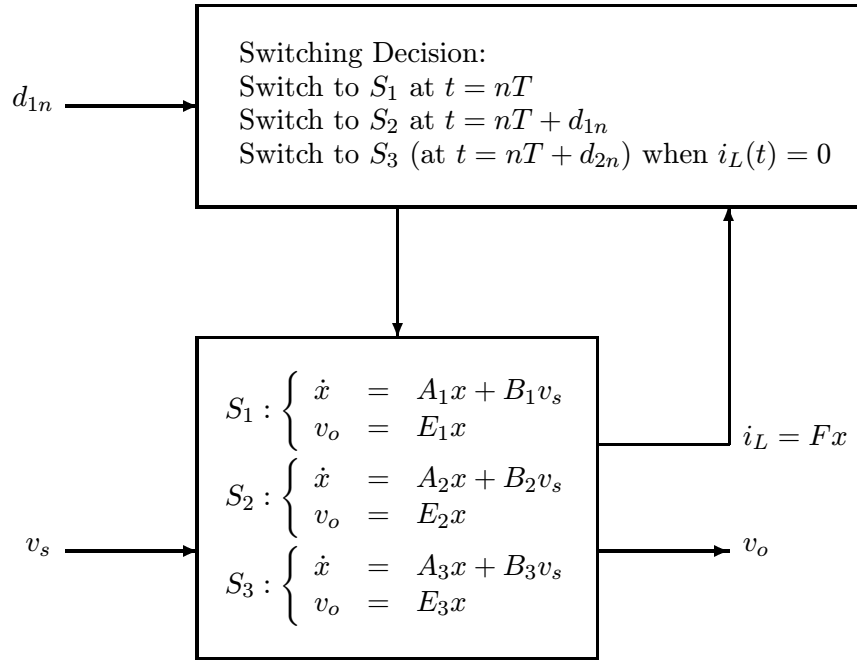
10

Figure 4: Power stage of PWM converter in DCM under voltage mode control

3.2 Nonlinear Sampled-Data Model

From the operation in Fig. 4, the sampled-data dynamics of the power stage is

$$
\begin{aligned}
x_{n+1} \;=\;& f(x_n, v_{sn}, d_{1n}, d_{2n}) \\[2mm]
=\;& e^{A_3(T-d_{2n})}\Big(e^{A_2(d_{2n}-d_{1n})}\big(e^{A_1 d_{1n}}x_n + \int_0^{d_{1n}} e^{A_1(d_{1n}-\sigma)}d\sigma B_1 v_{sn}\big) \\[2mm]
& + \int_{d_{1n}}^{d_{2n}} e^{A_2(d_{2n}-\sigma)}d\sigma B_2 v_{sn}\Big) + \int_{d_{2n}}^{T} e^{A_3(T-\sigma)}d\sigma B_3 v_{sn} \qquad (28)
\end{aligned}
$$

$$
\hat{v}_{on} \;=\; E\hat{x}_n \qquad (29)
$$

$$
\begin{aligned}
g(x_n, v_{sn}, d_{1n}, d_{2n}) \;=\;& Fx(nT+d_{2n}) \\[2mm]
=\;& F\big(e^{A_2(d_{2n}-d_{1n})}\big(e^{A_1 d_{1n}}x_n + \int_0^{d_{1n}} e^{A_1\sigma}d\sigma B_1 v_{sn}\big)\int_0^{d_{2n}-d_{1n}} e^{A_2\sigma}d\sigma B_2 v_{sn}\big) \\[2mm]
=\;& 0 \qquad (30)
\end{aligned}
$$

The variable d_{2n} is not a free variable but is constrained by Eq. (30). Another explicit constraint is $Fx_n = i_{Ln} = 0$, because the inductor current always starts from 0 at the beginning of a cycle.

11

Since $i_{Ln} = 0$ for any n, i_L is not a dynamic variable. Therefore, the dynamics is $(N-1)$-dimensional instead of N-dimensional.

3.3 Steady State Analysis

Let the nominal (set-point) output voltage be V_{SET}. The fixed point $(x_n, v_{sn}, d_{1n}, d_{2n}) = (x^0(0), V_s, d_1, d_2)$ of the sampled-data dynamics (28)-(30) should satisfy

$$x^0(0) \; = \; f(x^0(0), V_s, d_1, d_2) \tag{31}$$

$$V_{\mathrm{SET}} \; = \; Ex^0(0) \tag{32}$$

$$g(x^0(0), V_s, d_1, d_2) \; = \; 0 \tag{33}$$

Given the nominal (set-point) output voltage V_{SET} and $v_{sn} = V_s$, Newton's method can be used to solve these $(N+2)$ equations in $(N+2)$ unknowns (a fixed point:$(x^0(0), d_1, d_2)$).

3.4 Linearized Sampled-Data Dynamics

The system (28)-(30) can be linearized at the fixed point $(x^0(0), V_s, d_1, d_2)$. Using the notation $\diamond$ to denote evaluation at this fixed point,

$$\begin{aligned} \hat{x}_{n+1} &\approx \Phi_o \hat{x}_n + \Gamma_v \hat{v}_{sn} + \Gamma_d \hat{d}_{1n} \\ \hat{v}_{on} &= E\hat{x}_n \end{aligned} \tag{34}$$

where

$$\begin{aligned} \Phi_o &= \left. \frac{\partial f}{\partial x_n} - \frac{\partial f}{\partial d_{2n}} \Big(\frac{\partial g}{\partial d_{2n}}\Big)^{-1} \frac{\partial g}{\partial x_n} \right|_\diamond \\ &= e^{A_3(T-d_2)}\Big(I - \frac{(\dot{x}^0(d_2^-) - \dot{x}^0(d_2^+))F}{F\dot{x}^0(d_2^-)}\Big)e^{A_2(d_2-d_1)}e^{A_1 d_1} \end{aligned} \tag{35}$$

$$\begin{aligned} \Gamma_v &= \left. \frac{\partial f}{\partial v_{sn}} - \frac{\partial f}{\partial d_{2n}} \Big(\frac{\partial g}{\partial d_{2n}}\Big)^{-1} \frac{\partial g}{\partial v_{sn}} \right|_\diamond \\ &= e^{A_3(T-d_2)}\Big(e^{A_2(d_2-d_1)} \int_0^{d_1} e^{A_1\sigma} d\sigma B_1 + \int_0^{d_2-d_1} e^{A_2\sigma} d\sigma B_2\Big) + \int_0^{T-d_2} e^{A_3\sigma} d\sigma B_3 \end{aligned}$$

12

$$- \frac{\dot{x}^0(d_2^-) - \dot{x}^0(d_2^+)}{F\dot{x}^0(d_2^-)} F(e^{A_2(d_2-d_1)} \int_0^{d_1} e^{A_1\sigma} d\sigma B_1 + \int_0^{d_2-d_1} e^{A_2\sigma} d\sigma B_2) \tag{36}$$

$$\Gamma_d = \left. \frac{\partial f}{\partial d_{1n}} - \frac{\partial f}{\partial d_{2n}} \left(\frac{\partial g}{\partial d_{2n}} \right)^{-1} \frac{\partial g}{\partial d_{1n}} \right|_\diamond$$

$$= e^{A_3(T-d_2)} (I - \frac{(\dot{x}^0(d_2^-) - \dot{x}^0(d_2^+))F}{F\dot{x}^0(d_2^-)}) e^{A_2(d_2-d_1)} (\dot{x}^0(d_1^-) - \dot{x}^0(d_1^+)) \tag{37}$$

Since the dynamics is $(N-1)$-dimensional, the determinant of Φ_o is expected to be 0 (and hence a open-loop pole at 0). Indeed, from Eq. (35), one has

$$\det[\Phi_o] = \det[e^{A_2(d_2-d_1)} e^{A_1d_1} e^{A_3(T-d_2)}](1 - \frac{F(\dot{x}^0(d_2^-) - \dot{x}^0(d_2^+))}{F\dot{x}^0(d_2^-)}) = 0$$

because the inductor current is zero in the stage S_3 and hence $F\dot{x}^0(d_2^+) = \frac{d}{dt} i_L^0(d_2^+) = 0$.

3.5 A New Control-to-Output Transfer Function

Similar to Eq. (19) for CCM, the control-to-output transfer function in DCM is

$$T_{oc}(z) = \frac{\hat{v}_o(z)}{\hat{d}_1(z)} = E e^{A_1d_1} (zI - \Phi_o)^{-1} \Gamma_d + E\dot{x}^0(d_1^-) \tag{38}$$

4 Continuous Conduction Mode under Current Mode Control

The idea of using the sampled-data method to model current mode control has been proposed in [15, 36]. Here this approach is illustrated more explicitly and systematically.

4.1 Block Diagram Model

In current mode control, the control variable is a command signal v_c which sets the peak inductor current in a cycle. Consider the cycle $t \in [nT, (n+1)T]$. When the switching frequency is high, v_c can be set constant in a cycle, denoted as v_{cn} in the cycle. Denote by $h(t) = V_l + (V_h - V_l)(\frac{t}{T} \bmod 1)$ the slope-compensating ramp. The switch is turned on when a clock pulse occurs, and turned off

13

when the inductor current i_L reaches $v_{cn} - h(t)$. Denote by $nT + d_n$ the switching instant in the cycle when $i_L = v_{cn} - h(t)$, thus $i_L(nT + d_n) = v_{cn} - h(nT + d_n)$.

A general model of the power stage of a PWM converter operated in CCM under current mode control is shown in Fig. 5, where the matrix $F \in \mathbf{R}^{1 \times N}$ is chosen such that $Fx = i_L$. The remaining notation is the same as in Fig. 1.
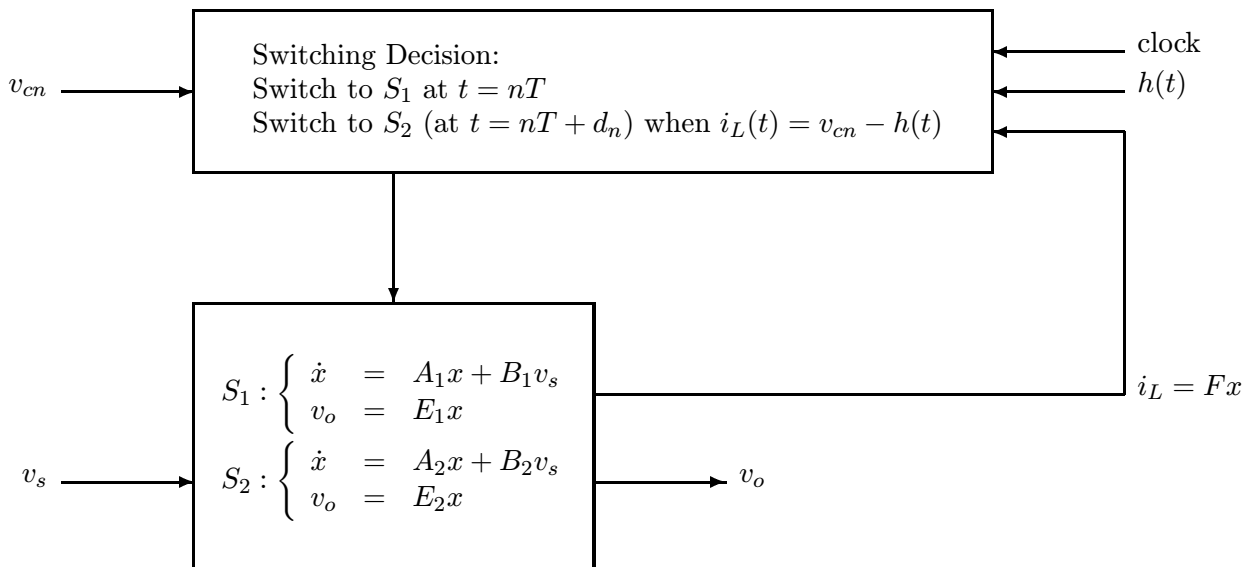

Figure 5: Power stage of PWM converter in CCM under current mode control

4.2   Nonlinear Sampled-Data Model

From Fig. 5 and the discussion above, the sampled-data dynamics of the power stage in CCM under current mode control is

$$
\begin{aligned}
x_{n+1} &= f(x_n, v_{sn}, d_n) \\
&= e^{A_2(T-d_n)}\left(e^{A_1 d_n} x_n + \int_0^{d_n} e^{A_1 \sigma} d\sigma B_1 v_{sn}\right) + \int_0^{T-d_n} e^{A_2 \sigma} d\sigma B_2 v_{sn} \\
v_{on} &= E x_n \\
g(x_n, v_{sn}, d_n, v_{cn}) &= i_L(nT + d_n) - (v_{cn} - h(nT + d_n)) \\
&= F\left(e^{A_1 d_n} x_n + \int_0^{d_n} e^{A_1 \sigma} d\sigma B_1 v_{sn}\right) - v_{cn} + h(d_n) \\
&= 0
\end{aligned}
\tag{39}
$$

Given the nominal (set-point) output voltage V_{SET} and $v_{sn} = V_s$, steady state analysis involves solving the set of $(N + 2)$ equations (Eq. (39)) with $(N + 2)$ unknowns (a fixed point $(x^0(0), d,$

$V_c))$.

4.3 Linearized Sampled-Data Dynamics

Assume there exists a fixed point $(x_n, v_{sn}, d_n, v_{cn}) = (x^0(0), V_s, d, V_c)$. Using the notation $\diamond$ to denote evaluation at this fixed point,

$$\hat{x}_{n+1} \approx \Phi_o \hat{x}_n + \Gamma_v \hat{v}_{sn} + \Gamma_c \hat{v}_{cn} \tag{40}$$

$$\hat{v}_{on} = E\hat{x}_n \tag{41}$$

where

$$\Phi_o = \left. \frac{\partial f}{\partial x_n} - \frac{\partial f}{\partial d_n}(\frac{\partial g}{\partial d_n})^{-1}\frac{\partial g}{\partial x_n} \right|_\diamond$$

$$= e^{A_2(T-d)}(I - \frac{(\dot{x}^0(d^-) - \dot{x}^0(d^+))F}{F\dot{x}^0(d^-) + \dot{h}(d)})e^{A_1 d} \tag{42}$$

$$\Gamma_v = \left. \frac{\partial f}{\partial v_{sn}} - \frac{\partial f}{\partial d_n}(\frac{\partial g}{\partial d_n})^{-1}\frac{\partial g}{\partial v_{sn}} \right|_\diamond$$

$$= e^{A_2(T-d)}(I - \frac{(\dot{x}^0(d^-) - \dot{x}^0(d^+))F}{F\dot{x}^0(d^-) + \dot{h}(d)}) \int_0^d e^{A_1\sigma} d\sigma B_1 + \int_0^{T-d} e^{A_2\sigma} d\sigma B_2 \tag{43}$$

$$\Gamma_c = \left. -\frac{\partial f}{\partial d_n}(\frac{\partial g}{\partial d_n})^{-1}\frac{\partial g}{\partial v_{cn}} \right|_\diamond$$

$$= \frac{e^{A_2(T-d)}(\dot{x}^0(d^-) - \dot{x}^0(d^+))}{F\dot{x}^0(d^-) + \dot{h}(d)} \tag{44}$$

The following result is related to a well-known stability criterion.

Theorem 3 *If the periodic solution $x^0(t)$ is open-loop asymptotically orbitally stable, then the following inequality holds:*

$$\left| \frac{F\dot{x}^0(d^+) + \dot{h}(d)}{F\dot{x}^0(d^-) + \dot{h}(d)} \right| \leq e^{\mathrm{tr}[A_2 - A_1]d - \mathrm{tr}[A_2]T} \tag{45}$$

Proof: Suppose the periodic solution $x^0(t)$ is open-loop asymptotically orbitally stable. Then all the eigenvalues of Φ have magnitude less than or equal than 1. Since $\det[\Phi]$ is the product of

the eigenvalues of Φ, we have that

$$
\begin{aligned}
|\det[\Phi]| &= \left| \det[e^{A_1 d} e^{A_2(T-d)}] \det[I - \frac{(\dot{x}^0(d^-) - \dot{x}^0(d^+))F}{F\dot{x}^0(d^-) + \dot{h}(d)}] \right| \\
&= \left| \det[e^{A_1 d} e^{A_2(T-d)}] \det[1 - \frac{F(\dot{x}^0(d^-) - \dot{x}^0(d^+))}{F\dot{x}^0(d^-) + \dot{h}(d)}] \right| \\
&= e^{-\text{tr}[A_2 - A_1]d + \text{tr}[A_2]T} \left| \frac{F\dot{x}^0(d^+) + \dot{h}(d)}{F\dot{x}^0(d^-) + \dot{h}(d)} \right| \\
&\leq 1
\end{aligned}
$$

Then Eq. (45) follows. $\qquad\qquad\qquad\qquad\qquad\qquad\qquad\qquad\qquad\qquad\qquad$ $\square$

Remark: Generally the switching period is so small that the right side of (45) can be approximated as 1, resulting in a condition that resembles a well-known stability criterion in current mode control [11, for example]:

$$
\left| \frac{-m_2 + m_c}{m_1 + m_c} \right| < 1 \tag{46}
$$

where m_1 is the (positive) slope of the *inductor current* trajectory during the on stage and $-m_2$ is the (negative) slope during the off stage using a *linear approximation* [1]; and $-m_c$ is the (negative) slope of the compensating ramp. The stability criterion (46) differs from Theorem 3, in which the *instantaneous* slope is used. Also, Theorem 3 applies to the *open-loop* system.

4.4 Control-to-Output Transfer Function

From the linearized dynamics (40) and (41), the control-to-output transfer function is

$$
T_{oc}(z) = \frac{\hat{v}_o(z)}{\hat{v}_c(z)} = E(zI - \Phi_o)^{-1}\Gamma_c \tag{47}
$$

16

5 A New "Lifted" Continuous-Time Power Stage Model Obtained from Sampled-Data Model

Two sampled-data dynamic models of the power stage have been derived, using the S (which uses sampled output $v_o(nT)$) and SP methods (which uses sampled output $v_o(nT + d_n)$). The sampled-data dynamics using the S method is useful for *discrete-time* controller design. The sampled-data dynamics using the SP method has better control-to-output frequency response, which is useful for *analog* controller design. Frequency response information suffices for the practical controller design. In some cases, continuous-time dynamical equations of the power stage are needed. For instance, such a model facilitates analog feedback control design for PWM converters. In this section, a new continuous-time model of the power stage will be derived for which the control-to-output frequency response is close to that of the sampled-data model. This continuous-time model differs from the traditional averaged model, which is independent of the switching frequency.

In obtaining the approximate continuous-time model from the sampled-data linearized model, it should be recognized that some of the benefits of sampled-data modeling are compromised. Most importantly, the duty cycle, which is best viewed as a function that changes in *discrete* steps from cycle to cycle, is viewed as a smooth function in *continuous-time*. The averaging method also uses such an approximate description of the duty cycle.

Given a linear sampled-data model, there are many ways to derive a continuous-time model with a similar frequency response [38]. Here one approach is proposed. Without loss of generality, such a continuous-time model will be obtained for the circuit operation in CCM under voltage mode control. The linearized sampled-data dynamics of the power stage using SP method is (11) with (18). Transforming ("lifting") the sampled-data pair $(\Phi_o, [\Gamma_v, \Gamma_d])$ to the continuous-time pair $(\Phi_o^c, [\Gamma_v^c, \Gamma_d^c])$ by the technique in Appendix A, the following continuous-time model of the power stage is proposed:

$$
\begin{aligned}
\dot{\hat{x}} &= \Phi_o^c \hat{x} + \Gamma_v^c \hat{v}_s + \Gamma_d^c \hat{d} \\
\hat{v}_o &= E e^{A_1 d} \hat{x} + E \dot{x}^0(d^-) \hat{d}
\end{aligned}
\tag{48}
$$

The control-to-output transfer function in the lifted dynamics (48) is

$$T_{oc}^c(s) = E e^{A_1 d}(sI - \Phi_o^c)^{-1} \Gamma_d^c + E \dot{x}^0(d^-) \tag{49}$$

6 Illustrative Examples

As mentioned in the Introduction, the main motivation for careful modeling of the power stage is to facilitate controller design. To verify the validity of power stage models, there are many approaches. One common approach involves using a dynamic analyzer to determine which model gives a frequency response most in agreement with experimental data. Here, another approach is used. Since *exact closed-loop* stability can be determined as shown in [29, 27], the exact gain margin can also be determined. Therefore, gain margin will be used to verify the validity of power stage models.

Generally the controller for a PWM converter uses dynamic feedback, with an integrator enclosed. For simplicity, static feedback is used. Accuracy of the sampled-data models will be illustrated by examples taken from the literature.

Example 1 (*Prediction of source voltage range for stable operation in a buck converter in CCM under voltage mode control with leading edge modulation*, [31]) Consider the buck converter under voltage mode control shown in Fig. 6. Let $T = 400\mu s$, $L = 20mH$, $C = 47\mu F$, $R = 22\Omega$, $V_r = 11.3V$, $g_1 = 8.4$, $V_l = 3.8V$, $V_h = 8.2V$, and $h(t) = V_l + (V_h - V_l)[\frac{t}{T} \mod 1]$. Note that in the leading edge modulation, S_1 is the off stage and S_2 is the on stage. The system has been shown to be unstable for $V_s > 24.527$ in [31] by computer simulation and in [39, 26] by closed-loop analysis.

However the system is predicted to be stable for $15 < V_s < 40$ if the averaging method is used [40].

In the following, the sampled-data method is used. It will be shown that the sampled-data model has better prediction of stability than the averaged model. Let the state $x = (i_L, v_C)'$, the

18

state matrices in Fig. 1 are

$$A_1 = A_2 = \begin{bmatrix} 0 & \frac{-1}{L} \\ \frac{1}{C} & \frac{-1}{RC} \end{bmatrix}$$

$$B_1 = \begin{bmatrix} 0 \\ 0 \end{bmatrix} \qquad\qquad B_2 = \begin{bmatrix} \frac{1}{L} \\ 0 \end{bmatrix}$$

$$E_1 = E_2 = \begin{bmatrix} 0 & 1 \end{bmatrix}$$

Take $V_s = 20$ for example. The duty cycle D_c can be estimated from the switching condition, $y(D_cT) = h(D_cT)$, or equivalently,

$$g_1(V_sD_c - V_r) = (1 - D_c)(V_h - V_l) + V_l$$

Solving this equation gives $D_c = 0.598$. Then $d = (1 - D_c)T = 1.6074 \times 10^{-6}$. From Eq. (19), the duty-ratio-to-output transfer function is $(-T)T_{oc}(z)$, where the negative sign is because of the leading edge modulation. The corresponding frequency response is shown in Fig. 7. The gain margin is 7.2 dB. The error amplifier and PWM modulator contribute a gain $g_1/(V_h - V_l) = 5.6165$ dB. Thus the gain which V_s can increase by [1] without causing instability is $7.2 - 5.6165 = 1.5835$ dB (1.20). This means that the system will be unstable for $V_s > 20 \times 1.20 = 24.0$. Therefore, sampled-data approach in this example has better prediction of closed-loop instability than the averaged method.

Example 2 (Prediction of gain margin of a boost converter in DCM under voltage mode control, [33]) The power stage of a boost converter is shown in Fig. 8, where the system parameters are $f_s = 3kHz$, $V_s = 16V$, $R = 12.5\Omega$, $L = 208\mu H$, $C = 222\mu F$, $R_c = 0$ and $V_{\text{SET}} = 25V$. The converter has been shown to be unstable for the feedback gain greater than 0.08 by simulation [33].

Let the state $x = (i_L, v_C)'$, the state matrices in Fig. 4 are

$$
A_1 = A_3 = \begin{bmatrix} 0 & 0 \\ 0 & \frac{-1}{RC} \end{bmatrix} \qquad A_2 = \begin{bmatrix} 0 & \frac{-1}{L} \\ \frac{1}{C} & \frac{-1}{RC} \end{bmatrix}
$$
$$
B_1 = B_2 = \begin{bmatrix} \frac{1}{L} \\ 0 \end{bmatrix} \qquad B_3 = \begin{bmatrix} 0 \\ 0 \end{bmatrix} \tag{50}
$$
$$
E_1 = E_2 = E_3 = \begin{bmatrix} 0 & 1 \end{bmatrix} \qquad F = \begin{bmatrix} 1 & 0 \end{bmatrix}
$$

---

[1]It can be seen from Eqs. (6) and (19) that V_s contributes linearly to the open-loop gain.
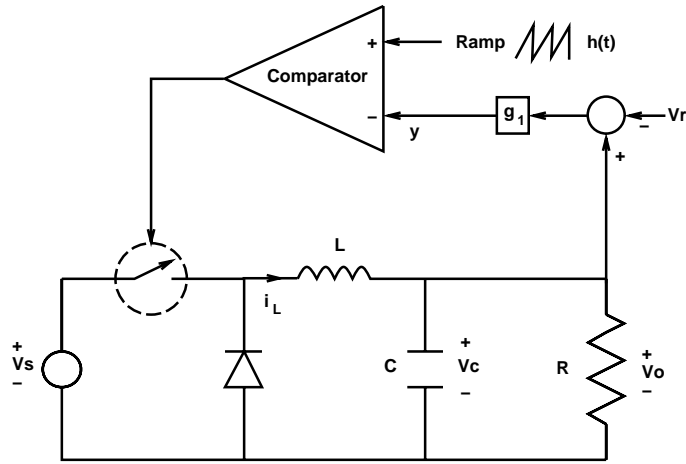
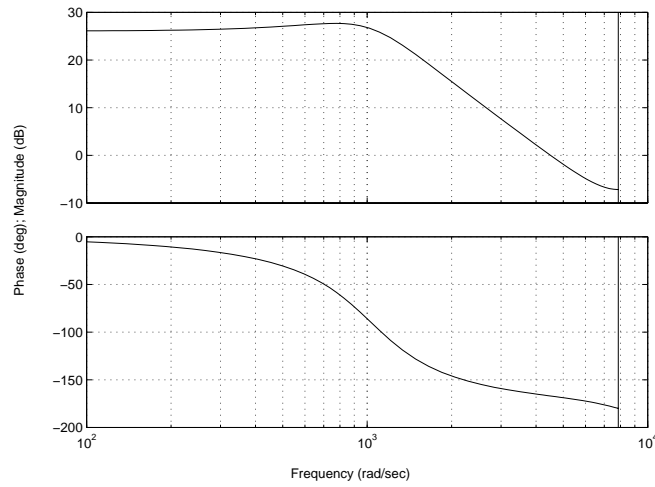Figure 6: System diagram for Example 1

Figure 7: Duty-ratio-to-output frequency response for Example 1

20

Solving Eqs. (31)-(33) by Newton's method gives $d_1 = 0.0001$ (hence $D_c = d_1 f_s = 0.3$) and $d_2 = 0.00027$.

From Eq. (38), the duty-ratio-to-output transfer function is $T_{oc}(z)T$. The corresponding frequency response is shown in Fig. 9. The gain margin is -22.66 dB (0.0736). So a feedback gain greater than 0.0736 is predicted to be destabilizing, which is close to the result of [33] noted above.

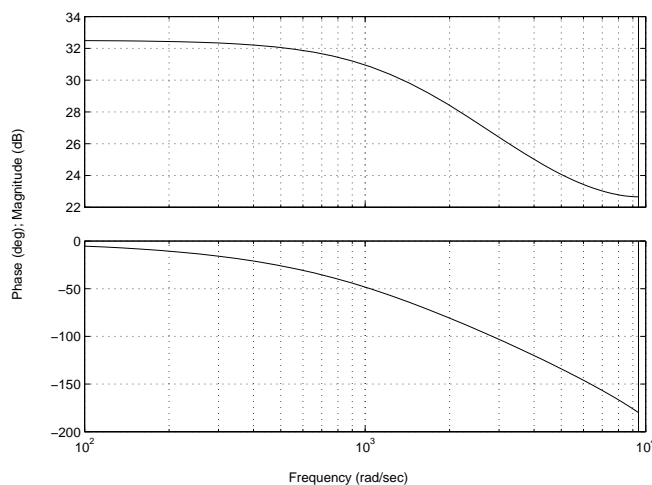Figure 8: Boost converter with source voltage and resistive load

Figure 9: Duty-ratio-to-output frequency response for Example 2

Example 3 (*Prediction of gain margin of a boost converter in DCM under voltage mode control,* [11, p.389]) The power stage of a boost converter is shown in Fig. 8, where the system parameters are $f_s = 100kHz$, $V_s = 24V$, $R = 12\Omega$, $L = 5\mu H$, $C = 470\mu F$, $R_c = 0$ and $V_{\mathrm{SET}} = 36V$.

In [11], two averaged models are used to study this circuit. One model is 1-dimensional, and its duty-ratio-to-output frequency response has infinite gain margin. The second model (based on [20]) has gain margin of 33 dB.

Next, consider the sampled-data model of this circuit. The state matrices in Fig. 4 are the same as in Eq. (50). Solving Eqs. (31)-(33) by Newton's method gives $d_1 = 2.5 \times 10^{-6}$ (hence $D_c = 0.25$), $d_2 = 7.4978 \times 10^{-6}$ and $x^0(d_1) = (i_L^0(d_1), v_C^0(d_1))' = (12, 35.98)'$. From Eq. (38), the duty-ratio-to-output transfer function is $T_{oc}(z)T$. The corresponding frequency response is shown in Fig. 10, from which the gain margin is found to be 9.91 dB.

To ascertain which of these models gives the best result, a feedback loop (Fig. 11) is added to the power stage. As the gain g varies, the nominal periodic solution $x^0(t)$ also varies. To keep the nominal periodic solution the same, the reference voltage is varied according to $V_r = \frac{h(d_1)}{g} + v_C^0(d_1) = \frac{0.25}{g} + 35.98$, a value close to 35.98 for different values of g. Using the exact closed-loop analysis in [29], the system is found to become unstable for gains $g > 3.13$ (9.91 dB). Thus the sampled-data model has given accurate prediction of the gain margin.
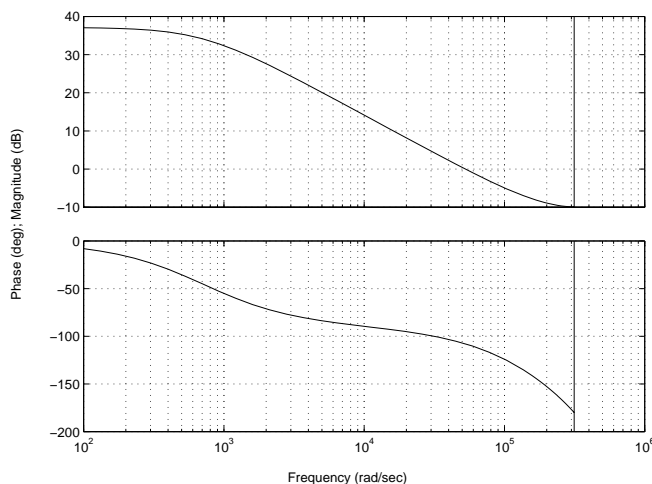

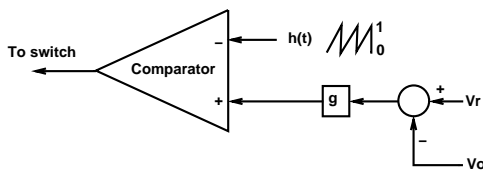Figure 10: Duty-ratio-to-output frequency response for Example 3

Figure 11: Simple static feedback for PWM converter under voltage mode control

Example 4 (*Prediction of gain margin of a boost converter in CCM under current mode control,* [18]) The power stage of a boost converter is shown in Fig. 8, where the system parameters are $f_s = 100kHz$, $V_s = 5V$, $R = 15\Omega$, $L = 40\mu H$, $C = 200\mu F$, $R_c = 0$ $V_h = 1$ and $V_c = 3$.

In [18], three averaged models are compared. The duty-ratio-to-output frequency response for each one has gain margin 29.7 dB, 29.7 dB and 29.6 dB, respectively.

Next the sampled-data model is applied. The matrices in Fig. 5 are the same as in Eq. (50). Calculating the fixed point in Eq. (39) gives $x^0(0) = (1.661, 12.3599)'$ and $x^0(d) = (2.4049, 12.3354)'$. From Eq. (47), the duty-ratio-to-output transfer function is $T_{oc}(z)T$. The corresponding frequency response is shown in Fig. 12. The gain margin is 28.2 dB (25.70).
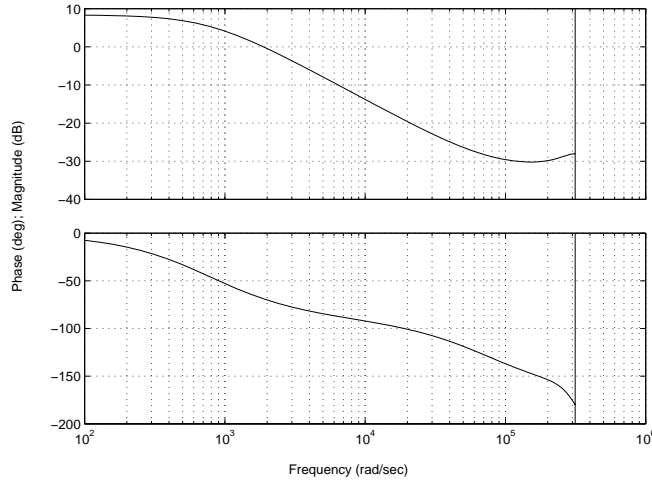

Figure 12: Duty-ratio-to-output frequency response for Example 4

A feedback loop (Fig. 13) is set up. As the gain g varies, the nominal periodic solution $x^0(t)$ also varies. To keep the nominal periodic solution the same, the reference voltage is varied according to $V_r = \frac{h(d)+i_L^0(d)}{g} + v_C^0(d) = \frac{3}{g} + 12.3354$. Using the exact closed-loop analysis in [29], the system is unstable for gains $g > 25.6803$ (28.192 dB). When $g = 25.6803$, the closed-loop eigenvalues are $0.3203 \pm 0.9474i$ (on the unit circle). Thus a Neimark-Sacker bifurcation [41, 26] occurs. It is surprising to see such a bifurcation occurring in a converter under current mode control.

From this example, the sampled-data model of the power stage predicts closed-loop instability

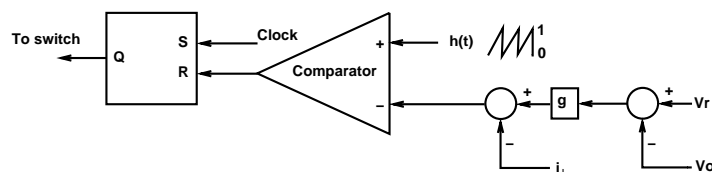more accurately than any of the three averaged models in [18].

Figure 13: Simple static feedback for PWM converter under current mode control

7   Concluding Remarks

Sampled-data models and associated analysis were developed for the power stage of the PWM DC-DC converter. Several configurations were considered, including DCM or CCM under voltage mode control, and CCM under current mode control. Compared with the derivations of averaged models in DCM or under current mode control, the sampled-data approach is more systematic. For each configuration, nonlinear and linearized sampled-data models, and control-to-output transfer function were derived. The frequency response obtained using the sampled-data models of this paper were found to be superior to those obtained using averaging. Insights were given on improving the accuracy of the computed phase response. In addition, a new ("lifted") continuous-time switching frequency-dependent model of the power stage was derived from the sampled-data model. Examples were used to illustrate the increased accuracy of controls designed using the new power stage models.

Acknowledgments

References

[1] R.D. Middlebrook and S. Ćuk, "A general unified approach to modelling switching-converter power stages," in *IEEE Power Electronics Specialists Conference Record*, 1976, pp. 18–34.

[2] A.R. Brown and R.D. Middlebrook, "Sampled-data modelling of switching regulators," in *IEEE Power Electronics Specialists Conference Record*, 1981, pp. 349–369.

[3] B.Y. Lau and R.D. Middlebrook, "Small-signal frequency response theory for piecewise-constant two-switched-network DC-to-DC converter systems," in *IEEE Power Electronics Specialists Conference Record*, 1986, pp. 186–200.

[4] B.Y. Lau and R.D. Middlebrook, "The small-signal behavior of ideal DC-to-DC switching convertors," in *IEEE International Symposium on Circuits and Systems*, 1987, pp. 998–1004.

[5] R. Tymerski, V. Vorperian, F.C.Y. Lee, and W.T. Baumann, "Nonlinear modeling of the PWM switch," *IEEE Transactions on Power Electronics*, vol. 4, no. 2, pp. 225–233, 1989.

[6] V. Vorperian, "Simplified analysis of PWM converters using model of PWM switch. I. Continuous conduction mode," *IEEE Transactions on Aerospace and Electronic Systems*, vol. 26, no. 3, pp. 490–496, 1990.

[7] R. Tymerski, "Frequency analysis of time-interval-modulated switched networks," *IEEE Transactions on Power Electronics*, vol. 6, no. 2, pp. 287–295, 1991.

[8] R. Tymerski, "Application of the time-varying transfer function for exact small-signal analysis," *IEEE Transactions on Power Electronics*, vol. 9, no. 2, pp. 196–205, 1994.

[9] J.O. Groves Jr., *Small Signal Analysis of Nonlinear Systems with Periodic Operating Trajectories*, Ph.D. thesis, Virginia Polytechnic Institute and State University, 1995.

[10] B. Lehman and R.M. Bass, "Switching frequency dependent averaged models for PWM DC-DC converters," *IEEE Transactions on Power Electronics*, vol. 11, no. 1, pp. 89–98, 1996.

[11] R.W. Erickson, *Fundamentals of Power Electronics*, Chapman and Hall, New York, 1997.

[12] C.-C. Fang and E.H. Abed, "Sampled-data modeling and analysis of PWM DC-DC converters II. The power stage," Tech. Rep. 98-55, Institute for Systems Research, University of Maryland, College Park, 1998, available at http://www.isr.umd.edu/TechReports/ISR/1998/.

[13] S.-P. Hsu, A. Brown, L. Rensink, and R.D. Middlebrook, "Modelling and analysis of switching DC-to-DC converters in constant-frequency current-programmed mode," in *IEEE Power Electronics Specialists Conference Record*, 1979, pp. 284–301.

[14] R.D. Middlebrook, "Topics in multiple-loop regulators and current-mode programming," in *IEEE Power Electronics Specialists Conference Record*, 1985, pp. 716–732.

[15] G.C. Verghese, C.A. Bruzos, and K.N. Mahabir, "Averaged and sampled-data models for current mode control: a re-examination," in *IEEE Power Electronics Specialists Conference Record*, 1989, pp. 484–491.

[16] R.B. Ridley, "A new, continuous-time model for current-mode control," *IEEE Transactions on Power Electronics*, vol. 6, no. 2, pp. 271–280, 1991.

[17] F.D. Tan and R.D. Middlebrook, "A unified model for current-programmed converters," *IEEE Transactions on Power Electronics*, vol. 10, no. 4, pp. 397–408, 1995.

[18] J. Sun and R. Bass, "A new approach to averaged modeling of PWM converters with current-mode control," in *Proc. of International Conference on Industrial Electronics, Control, and Instrumentation*, 1997.

[19] S. Ćuk and R.D. Middlebrook, "A general unified approach to modelling switching DC-to-DC converters in discontinuous conduction mode," in *IEEE Power Electronics Specialists Conference Record*, 1977, pp. 36–57.

[20] V. Vorperian, "Simplified analysis of PWM converters using model of PWM switch. II. Discontinuous conduction mode," *IEEE Transactions on Aerospace and Electronic Systems*, vol. 26, no. 3, pp. 497–505, 1990.

[21] D. Maksimovic and S. Cuk, "A unified analysis of PWM converters in discontinuous modes," *IEEE Transactions on Power Electronics,*, vol. 6, no. 3, pp. 476–490, 1991.

[22] J. Sun, D.M. Mitchell, M. Greuel, P.T. Krein, and R.M. Bass, "Modeling of PWM converters in discontinuous conduction mode - A reexamination," in *IEEE Power Electronics Specialists Conference Record*, 1998.

[23] F.C.Y. Lee, R.P. Iwens, Yuan Yu, and J.E. Triner, "Generalized computer-aided discrete time-domain modeling and analysis of DC-DC converters," *IEEE Transactions on Industrial Electronics and Control Instrumentation*, vol. IECI-26, no. 2, pp. 58–69, 1979.

[24] G.C. Verghese, M. Elbuluk, and J.G. Kassakian, "A general approach to sample-data modeling for power electronic circuits," *IEEE Transactions on Power Electronics*, vol. 1, no. 2, pp. 76–89, 1986.

[25] R. Lutz and M. Grotzbach, "Straightforward discrete modelling for power converter systems," in *IEEE Power Electronics Specialists Conference Record*, 1986, pp. 761–770.

[26] C.-C. Fang, *Sampled-Data Analysis and Control of DC-DC Switching Converters*, Ph.D. thesis, University of Maryland, College Park, 1997, available at http://www.isr.umd.edu/TechReports/ISR/1997/.

[27] C.-C. Fang and E.H. Abed, "Sampled-data modeling and analysis of closed-loop PWM DC-DC converters," to appear at *IEEE International Symposium on Circuits and System*, May 1999.

[28] J.L. Duarte, "Small-signal modelling and analysis of switching converters using matlab," *International Journal of Electronics*, vol. 85, no. 2, pp. 231–269, 1998.

[29] C.-C. Fang and E.H. Abed, "Sampled-data modeling and analysis of PWM DC-DC converters I. Closed-loop circuits," Tech. Rep. 98-54, Institute for Systems Research, University of Maryland, College Park, 1998, available at http://www.isr.umd.edu/TechReports/ISR/1998/.

[30] J.H.B. Deane and D.C. Hamill, "Instability, subharmonics, and chaos in power electronics circuits," *IEEE Transactions on Power Electronics*, vol. 5, no. 3, pp. 260–268, 1990.

[31] D.C. Hamill, J.H.B. Deane, and J. Jefferies, "Modeling of chaotic DC-DC converters by iterated nonlinear mappings," *IEEE Transactions on Power Electronics*, vol. 7, no. 1, pp. 25–36, 1992.

[32] J.H.B. Deane, "Chaos in a current-mode controlled boost DC-DC converter," *IEEE Transactions on Circuits and Systems-I: Fundamental Theory and Applications*, vol. 39, no. 8, pp. 680–683, 1992.

[33] C.K. Tse, "Flip bifurcation and chaos in three-state boost switching regulators," *IEEE Transactions on Circuits and Systems-I: Fundamental Theory and Applications*, vol. 41, no. 1, pp. 16–23, 1994.

[34] F. Garofalo, P. Marino, S. Scala, and F. Vasca, "Control of DC-DC converters with linear optimal feedback and nonlinear feedforward," *IEEE Transactions on Power Electronics*, vol. 9, no. 6, pp. 607–615, 1994.

[35] C.-C. Fang and E.H. Abed, "Discrete-time integral control of PWM DC-DC converters," Tech. Rep. 98-52, Institute for Systems Research, University of Maryland, College Park, 1998, available at http://www.isr.umd.edu/TechReports/ISR/1998/.

[36] J.G. Kassakian, M.F. Schlecht, and G.C. Verghese, *Principles of Power Electronics*, Addison-Wesley, Reading, MA, 1991.

[37] A.V. Oppenheim and R.W. Schafer, *Discrete-Time Signal Processing*, Prentice-Hall, Englewood Cliffs, NJ, 1989.

[38] G.F. Franklin, D. Powell, and M.L. Workman, *Digital Control of Dynamic Systems*, Addison-Wesley, Reading, Mass., Second edition, 1990.

[39] E. Fossas and G. Olivar, "Study of chaos in the buck converter," *IEEE Transactions on Circuits and Systems-I: Fundamental Theory and Applications*, vol. 43, no. 1, pp. 13–25, 1996.

[40] D.C. Hamill, "Power electronics: A field rich in nonlinear dynamics," in *Nonlinear Dynamics of Electronic Systems*, Dublin, 1995.

[41] Y.A. Kuznetsov, *Elements of Applied Bifurcation Theory*, Springer-Verlag, New York, 1995.

Appendix A Discretizing a Continuous-Time System Through a Zero-Order-Hold

Consider a linear continuous-time system

$$\begin{aligned} \dot{x} &= Ax + Bu \\ y &= Ex \end{aligned} \tag{51}$$

where $A \in \mathbf{R}^{N \times N}$, $B \in \mathbf{R}^{N \times 1}$, $E \in \mathbf{R}^{1 \times N}$, $x \in \mathbf{R}^{N}$, and $y, u \in \mathbf{R}$.

To obtain a discrete-time model from this continuous-time system, a zero-order-hold is inserted before the input signal, and the output is sampled using a sampling interval T equal to the duration of the zero-order-hold; see Fig. 14. This involves an assumption that the input varies slowly enough to be considered constant within intervals of length T.
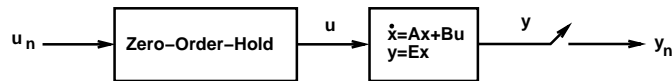

Figure 14: Discretizing a continuous-time system through a zero-order-hold

The discrete-time system has the dynamics

$$\begin{aligned} x_{n+1} &= \Phi x_n + \Gamma u_n \\ y_n &= Ex_n \end{aligned} \tag{52}$$

where

$$\Phi = e^{AT} \tag{53}$$

$$\Gamma = \int_0^T e^{A\sigma} d\sigma B \tag{54}$$

27

The following fact facilitates converting back to the the continuous-time pair (A, B) from knowledge of the discrete-time pair (Φ, Γ) and T. This process of converting back may be thought of as "lifting" the discrete-time dynamics to obtain a consistent continuous-time system.

Fact 1

$$\left[\begin{array}{cc} \Phi & \Gamma \\ 0 & 1 \end{array} \right] = \exp(\left[\begin{array}{cc} A & B \\ 0 & 0 \end{array} \right] T)$$

The input-to-output transfer function in the continuous-time domain is

$$E(sI - A)^{-1}B \tag{55}$$

The input-to-output transfer function in the discrete-time domain is

$$E(zI - \Phi)^{-1}\Gamma \tag{56}$$

Given the discrete-time dynamics (52) and the value of T, the continuous-time transfer function (55) can be obtained by using Fact 1.